A Practical System Approach for Fully Autonomous Multi-Dimensional Structural Health Monitoring

Jeong Ki Kim[1a], Dao Zhou[a], Dong Sam Ha[a], and Daniel Inman[b]
[a]Center for Embedded Systems for Critical Applications (CESCA)
Department of Electrical and Computer Engineering, Virginia Tech, Blacksburg, VA 24061
[b]Center for Intelligent Material Systems and Structures (CIMSS)
Virginia Tech, 310 Durham Hall MC 0261, Blacksburg, VA 24061

ABSTRACT

We present an SHM system integrating both the impedance and the Lamb wave propagation method on a single board, while sharing the same DSP (Digital Signal Processing) processor and the piezoelectric patches. Three functional blocks, such as signal excitation/generation, signal sensing, and data processing, were implemented to incorporate the Lamb wave method into our existing impedance-based SHM system. Both pitch-and-catch and pulse-and-echo schemes were implemented for damage detection and location, respectively. Through synergetic integration of the two methods, our SHM system can detect various types of simulated damages on aluminum plates.

Keywords: structural health monitoring, structural damage detection, impedance method, Lamb wave, wave propagation method, digital signal processor, discrete wavelet transform

1. INTRODUCTION

A major focus of the structural health monitoring (SHM) community is to incorporate SHM technologies into real world structures. A smaller form-factor is highly desirable for the purpose, as it increases the physical robustness and lowers the manufacturing and deployment cost. To detect or locate various types of defects such as incipient cracks, notches, fractures, and loose joints, it necessitates an SHM system to employ different SHM methods [1]. However, most existing SHM systems employ only one type of SHM methods targeting specific damages [2][3]. To cover different types of damages, we need multiple such SHM systems, resulting in an increased form factor and the cost.

An impedance-based SHM system performs three major operations: excitation signal generation, sensing the response signal, and damage assessment. The excitation signal for existing SHM systems is typically a sweeping sinusoidal signal, which is generated with a digital-to-analog converter (DAC). The response signal is captured by an analog-to-digital converter (ADC) and is processed by a DSP chip. Existing systems are complicate and power hungry due to employing an ADC, a DAC and a complex DSP processor. To address the problems, we proposed a new impedance-based SHM method, which performs SHM operations in the digital domain [4]. Our system excites a PZT (Lead Zirconate Titanate) patch with a train of rectangular pulses instead of a sinusoidal signal, which eliminates a DAC. Our system senses only the phase, not the magnitude, of the response signal to eliminate an ADC. Therefore, our system is much simpler in hardware and dissipates far less power.

The Lamb wave propagation method launches an elastic wave through the structure. The changes in both wave attenuation and reflection are sensed to detect and locate damages on surfaces [5][6]. Since both the impedance and the Lamb wave methods can share a processor and piezoelectric patches, we incorporated the Lamb wave method, both pitch-and-catch and pulse-and-echo schemes, into our SHM system. A Hanning windowed sinusoidal signal is generated to excite a Lamb wave for our system. A Hanning windowed sinusoidal signal has a small frequency bandwidth [7], so the generated Lamb waves are limited to fundamental modes. We applied a discrete wavelet transform to the sensed response, which reduces processing complexity and the memory requirement compared with other transformations such as FFT. Our integrated SHM system successfully detects various types of simulated damages on aluminum plates.

[1] jeongki@vt.edu, phone: (540) 231-2424, fax: (540) 231-3362, www.cesca.us

Sensors and Smart Structures Technologies for Civil, Mechanical, and Aerospace Systems 2009
edited by Masayoshi Tomizuka, Chung-Bang Yun, Victor Giurgiutiu, Proc. of SPIE Vol. 7292
72921L · © 2009 SPIE · CCC code: 0277-786X/09/$18 · doi: 10.1117/12.816289

This paper is organized as follows. Section 2 describes our impedance-based SHM system, and Section 3 describes design of the Lamb wave propagation method. Section 4 presents integration of the two methods on a single DSP board. Section 5 presents experimental results for the Lamb wave method, and Section 6 draws conclusions from our work.

2. IMPEDANCE-BASED DIGITAL SHM SYSTEM

The impedance method has many advantages over other damage detection methods. The small wavelengths at high frequencies allow the impedance method to detect minor changes in structural integrity. The impedance method can monitor the interior of complex structures, is very sensitive to changes in structural integrity, and often detects incipient damage at a far earlier stage than alternative systems [8]. We describe our impedance-based SHM system, into which the Lamb wave method was incorporated.

2.1. System Operation and Architecture

Major differences for our digital impedance-based SHM system from traditional systems lie in the excitation signal and sensing the response. Our system excites a PZT with a train of rectangular pulses instead of a sinusoidal signal and measures the phase of the response signal instead of the magnitude. Figure 1 (a) shows a pulse train, whose pulse repetition period or the fundamental frequency changes to sweep the target frequency range. Use of a pulse train simplifies the excitation signal generation and eliminates a DAC. A pulse train introduces harmonic terms as shown in Figure 1 (b) and (c). Harmonic terms would not cause a problem in practical sense, as they would cause the same effect for healthy and damaged structures.

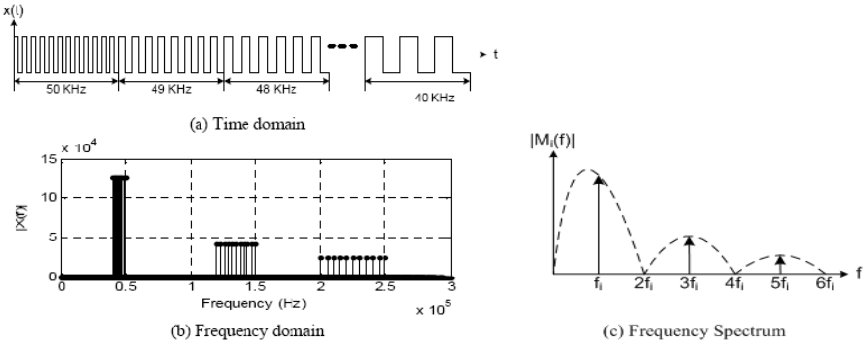

Figure 1: Excitation Signal for Our Digital SHM System

The electrical admittance of a PZT patch can be expressed as $Y(jf) = G(f) + jB(f)$, where $G(f)$ and $B(f)$ are conductance and susceptance terms, respectively. It is known that the conductance term is more sensitive to damages [8][9]. Let $G_{base}(f)$ denote as the baseline conductance obtained from a healthy structure and $G_{SUT}(f)$ as the conductance of the structure under test (SUT). The difference between the baseline and the SUT conductance, $G_{base}(f) - G_{SUT}(f)$, indicates a damage of the structure under test. The following relationship is shown in [10].

$$G_{base}(f) - G_{SUT}(f) = k \sin[\phi_{base}(f) - \phi_{SUT}(f)] \tag{1}$$

where k is approximately a constant, and $\phi_{base}(f)$ *and* $\phi_{SUT}(f)$ are the phase of $Y_{base}(f)$ and $Y_{SUT}(f)$, respectively. Expression (1) suggests that the phase difference can be used to assess a damage of a structure instead of measuring $G(f)$ directly. Our digital SHM system measures the phase difference, specifically the time difference between the voltage and the current exerted to the structure. The measurement of the phase difference eliminates an analog-to-digital converter (ADC) and an FFT (Fast Fourier Transform) operation, which simplifies the complexity of the system in hardware and computation.

The excitation and sensing part of our SHM system is shown in Figure 2. A digital signal processing (DSP) generates a train of rectangular pulses, which is applied to a PZT patch. The opamp output voltage $V_o(t)$, which represents the current through the PZT patch, is converted into a binary signal by the comparator. The binary signal and the input voltage $V_i(t)$ are compared using an exclusive-OR (XOR) gate to measure the phase difference of the two signals, i.e., the voltage and the current of the PZT patch.

More specifically, a train of pulses with each fundamental frequency f is applied for 10 ms. The XOR gate continuously compares the input voltage $V_i(t)$ and the binary signal of the output voltage $V_o(t)$. The output (either 1 or 0) of the XOR gate is sampled at the rate of 100 kHz, and its value is accumulated. It can be seen easily that the resultant accumulated value is $N\phi(f)$, where N is a constant depending on the sampling rate and duration of the train of pulses. The constant N is 160 for our SHM system. In order to avoid use of fractional numbers, the phase $\phi(f)$ is represented as an integer value $N\phi(f)$ for our system hereafter.

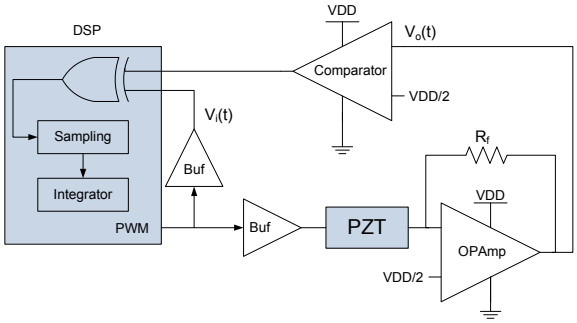

Figure 2: Excitation and Sensing Part of Our SHM System

2.2. Phase Profile and Damage Metric

The excitation frequency f is swept from the target frequency range from f_l to f_h noted with increment of 0.12 kHz. The phase profile of a structure represents a set of phase values $\phi(f_i)$'s, where f_i is discrete values between the frequency range f_l to f_h with increment of 0.12 kHz. As noted above, we use an integer value to represent a phase $\phi(f_i)$ instead of the actual phase value.

The damage metric (DM) for our system is defined as an *absolute sum of difference (ASD)* between the baseline and the SUT phase profiles and is calculated as below.

$$\mathrm{DM} = \sum_{f=f_1}^{f_2} \left| \phi_{base}(f) - \phi_{SUT}(f) \right| \quad \textbf{(2)}$$

The DM is compared against a threshold value, which may be set based on field experience. If DM is lower than the threshold value, the SUT is considered healthy. Otherwise, it is considered as damaged.

2.3. Prototyping of Our Digital SHM System

Figure 3 shows a prototype developed with a DSP evaluation board (TMS320F2812 from Texas Instruments) and a breadboard for the interface circuit such as opamps. Since our system does not require any ADC and DAC, our system is compact and power efficient.

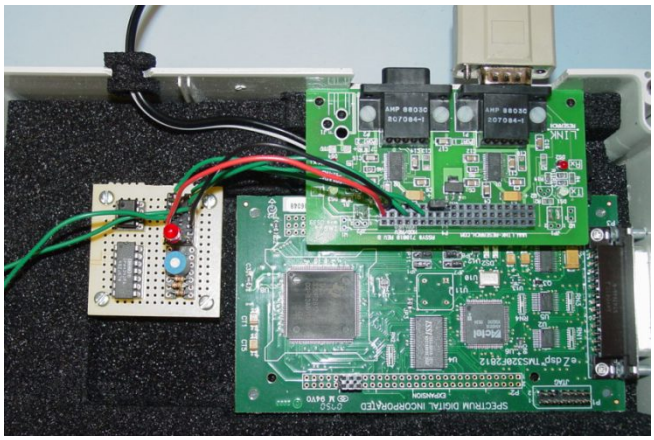

Figure 3: Prototype of Our Digital SHM System

3. DESIGN AND IMPLEMENTATION OF A LAMB WAVE METHOD

In order to implement the Lamb wave propagation method, various design parameters should be taken into consideration. We briefly describe design and implementation issues for the Lamb wave method.

3.1. Excitation Signal Generation

The first step for the system design procedure for the Lamb wave method is to select an optimal driving frequency and shape of the excitation signal for a structure. The excitation frequency should be as low as possible in order to avoid multiple higher modes in the driving frequency range. At the same time, the excitation frequency should be high enough to make the wavelength of the Lamb wave comparable to the scale of local damage. The slope of the group velocity curve need to be close to zero because a steep slope of the phase velocity makes it difficult to maintain a constant velocity of the Lamb wave through the material [5][11]. To balance the criteria for the dispersion curve, a few experiments are necessary to find the optimal driving frequency range.

The shape of the excitation waveform also plays a crucial role. One of the most widely used excitation waveforms is a tone burst of sine wave with Hanning (equivalently raised-cosine with roll-off factor = 1) window. Figure 4 (a) and (b) show a Hanning windowed 200 kHz sine wave with four peaks in time domain, which is the excitation signal for our experiments.

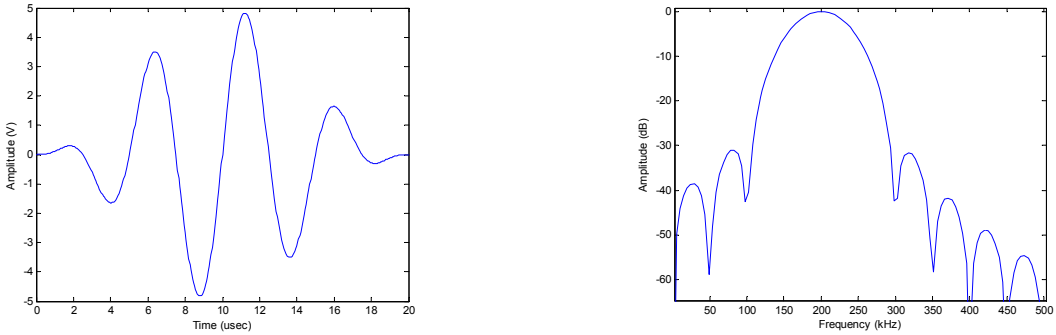

(a) Excitation Waveform at 200 kHz (b) Normalized Frequency Spectrum

Figure 4: Hanning Windowed Sine Wave with Four Peaks

3.2. Signal Processing for Damage Assessment

The key to reliable and high-resolution damage detection is good signal interpretation, and wavelet transform technique has been widely used [12][13]. We used discrete wavelet transform (DWT) to enhance Lamb wave signals in a noisy environment. DWT is a special case of the wavelet transform that provides a compact representation of a signal in time and frequency, and it can be computed efficiently. DWT is defined in the following expression:

$$W_{\Psi}(j,k) = \sum_{j}\sum_{k} s(n)2^{-j/2}\Psi_{j,k}(2^{-j}n-k)$$

where $\Psi_{j,k}$ is called as mother wavelet with finite energy. The flexibility of choosing a proper mother wavelet is one of the strongest advantages of using DWT. If we choose the mother wavelet as the excitation signal itself and the dilation coefficient j = 0, the DWT results in the correlation between the excitation signal and the sensed signal, which is simple to compute.

The detection metric (DM) used for our system is a normalized absolute sum of difference between the DWT of the baseline or reference signature and the DWT of the sensed signature from the structure under test. The DM indicates the amount of deviation of the sensed signature from the baseline. The DM increases with the damage level and is ideally zero for a structure without damage. The DM is expressed as follow:

$$DM = \frac{\sum_{i}\left|WT_{current}(i) - WT_{baseline}(i)\right|}{\sum_{i}\left|WT_{baseline}(i)\right|}$$

where WT_{current} and WT_{baseline} denote DWT of the sensed and baseline waveforms, respectively. $|x|$ denotes the absolute value of x.

3.3. Implementation of the Lamb Wave Method

Our system for the Lamb wave method comprises three functional blocks: a processing unit, a signal actuation unit, and a signal sensing unit as shown in Figure 5. The processing unit is a DSP EVM (TMS320F2812 from Texas Instruments). It controls the overall test procedure and performs excitation signal generation and damage assessment. The signal sensing unit consists of a DAC and opamps. The DAC module (THS5661 EVM from Texas Instruments) has 12-bit resolution and maximum conversion rate of 100 MSPS. The DAC module generates analog excitation signals, whose signal strength is boosted with opamps to increase the signal to noise ratio.

The propagated Lamb waves sensed at a PZT patch are amplified by opamps at the sensing unit. The sensing unit also adjusts the signal level to fit the input range of the ADC residing in the DSP core chip. The ADC has a 12-bit resolution with a built-in sample-and-hold circuit. The ADC is configured to operate at 8.3 MSPS for our system. The sensed digital data is stored in the memory on the DSP DVM for further processing.

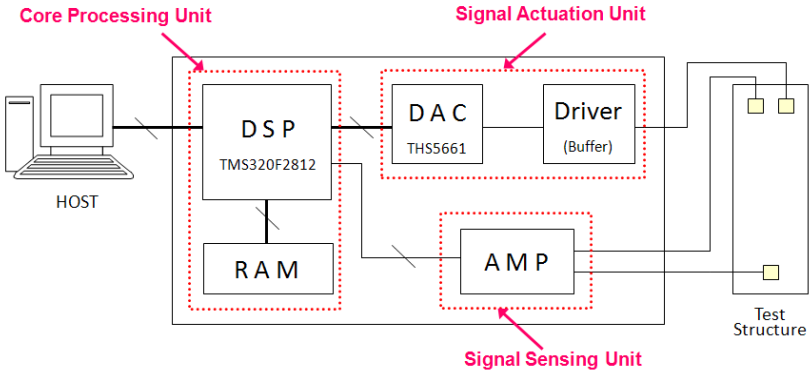

Figure 5: System Architecture for the Lamb Wave Method

4. INTEGRATION OF THE TWO METHODS

The overall system block diagram is shown in Figure 6. The core processing unit is shared by both methods along with the PZT patches attached to the structure. The upper half of the functional blocks is for the Lamb wave method. The DSP generates and applies a Hanning windowed digital waveform (stored at the look-up table) to the DAC, which converts it to an analog Lamb wave. The sensed waveform from the PZT patch is amplified and converted into digital data for further processing.

The lower half of the block diagram is for the impedance-based SHM. The DSP EVM generates a train of rectangular pulses, whose signal strength is boosted with opmps. The sensed waveform is converted into a digital signal by a comparator and applied to the DSP.

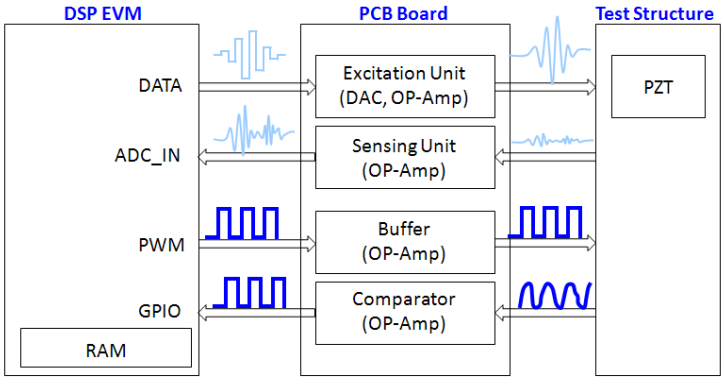

Figure 6: Overall Architecture for Combined Methods

Our final SHM system integrating the two methods is shown in Figure 7. It consists of three boards and has the dimension of 8.6 cm × 13.5 cm × 6.1 cm (W × L × H).

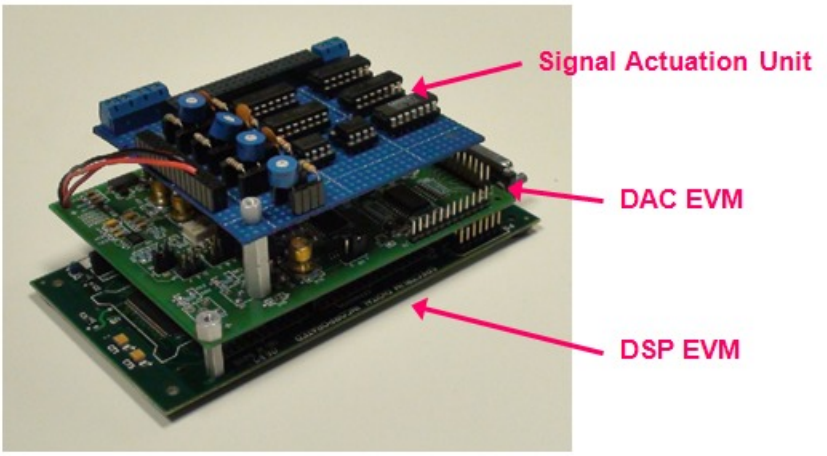

Figure 7: Our SHM System for Combined Methods

5. EXPERIMENTAL RESULTS AND OBSERVATIONS

Experimental results for our impedance-based digital SHM system are reported already in [4][14]. So, we present experimental results only for the Lamb wave propagation method in the following.

5.1. Experiment Setup

In order to validate the performance of our system, we used an aluminum alloy plate for the test structure as shown in Figure 8. The plate is 36 inch × 36 inch × 0.063 inch and mounted with four PZT patches in a square grid pattern with 12 inch apart with each other as indicated in Figure 9. Each PZT patch is circular with 0.5 inch in diameter and 0.01 inch thick. Each PZT patch was bonded with super glue with some pressure applied until hardened.

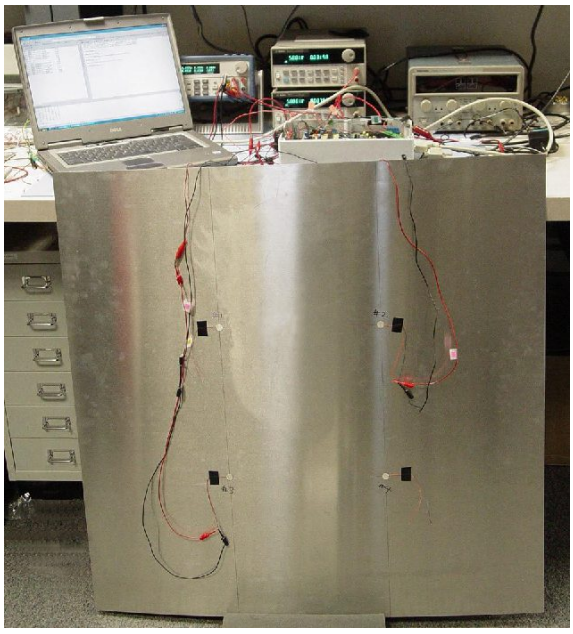

Figure 8: Test Set-up

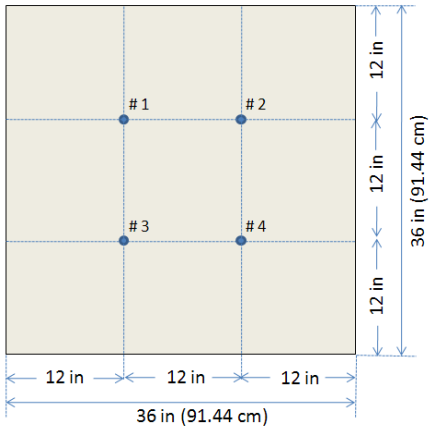

Figure 9: Dimension of the Plate

Five different damages as shown in Figure 10 were considered to test the Lamb wave method. The first damage is removable putty, which was placed between PZT #1 and #2. The putty adds local mass and changes boundary conditions that will alter the propagation of Lamb waves (Figure 10 (a)). Then, the putty was removed, and a notch was introduced at the location (Figure 10 (b)). Then, the notch was replaced with a thick cut (Figure 10 (c)). The above three damages were introduced successively and the Lamb wave method was tested for each damage introduced. The fourth damage is a hole with a 0.23 inch in diameter between PZT #1 and #3 (Figure 10 (d)). The fifth damage is a cut located at 2.3 inch below PZT #4 along the extension of the path between PZT #2 and #4, and the damage was intended for testing the pulse-and-echo method (Figure 10 (e)). The cuts in Figure 10 (c) and Figure 10 (e) are almost identical except their locations.

(a) Putty between PZT #1 and #2

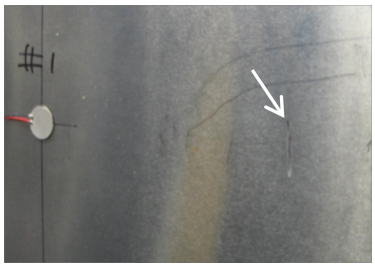

(b) Notch between PZT #1 and #2

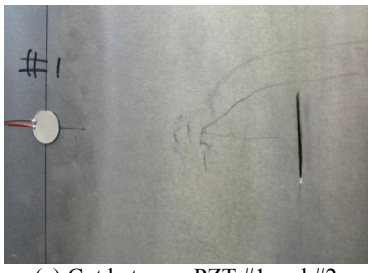

(c) Cut between PZT #1 and #2

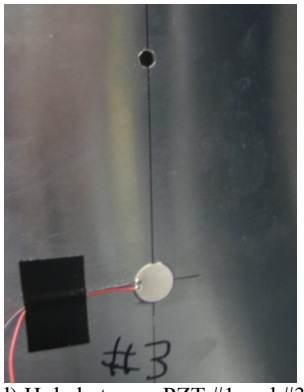

(d) Hole between PZT #1 and #3

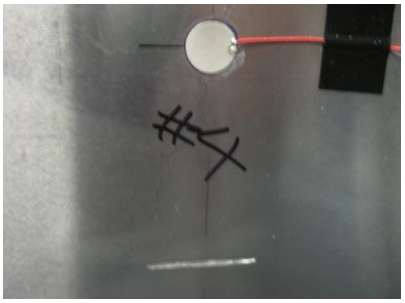

(e) Cut below PZT #4

Figure 10: Five Different Damages Introduced to the Plate

5.2. Experimental Results

Pitch-and-Catch Experiments:

The excitation signal for our experiments is a Hanning-windowed 200 kHz sinusoidal waveform shown in Figure 4 (a), and the signal has four cycles of the sinusoidal signal and lasts for 20 μs. The excitation frequency of 200 kHz was chosen for a good separation of the fundamental synchronous mode S_0 from the fundamental asynchronous mode A_0. The excitation signal was applied to a PZT patch of the healthy structure in pristine, and the response was captured at another PZT patch. Specifically, the response was sampled for 0.5 msec by the ADC with the sample rate of 8.3 MSPS and the resolution of 12 bits. The sampled data with size of 4 K bytes was stored in a memory. The same process was repeated eight times, and the arithmetic average of the eight responses is the final baseline waveform. Figure 11 (a) shows a baseline waveform for the PZT #1 as an actuator and PZT #2 as a sensor. Figure 11 (b) is the discrete wavelet transform of the baseline profile, which suppresses noise and the DC offset of the original waveform.

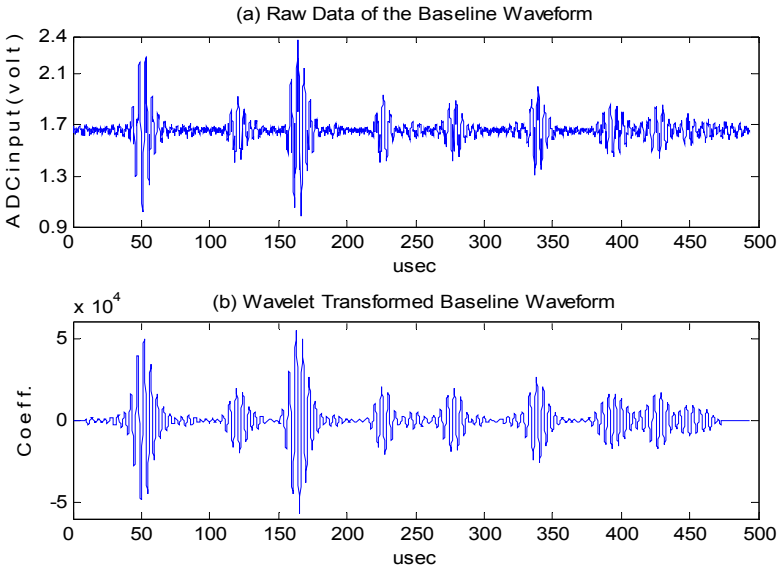

Figure 11: Baseline Waveforms as PZT #2 as Actuator and PZT #4 as Sensor

The first tone burst arrived at 50 μs in Figure 11 is the fundamental modes S_0 through the direct path between PZT #1 and PZT #2, and the second burst arrived at 120 μs is the fundamental asynchronous mode A_0. All other signals are reflected ones from boundaries of the plate. The propagation speed of the S_0 and the A_0 modes is obtained as about 5080 m/sec and 2350 m/sec, respectively.

Once the baseline waveform was obtained, we experimented with damaged structures. Figure 12 shows attenuations of the Lamb waves for the fundamental mode S_0 under the putty damage in Figure 10 (a) and the cut damage in Figure 10 (c). It is noticeable that the putty damage incurs more attenuation than the cut damage. The DMs for the first four damages in Figure 10 (a) – (d) are tabulated in Table 1. The cut damage is the severest in terms of DM and the notch damage the mildest. Noting that the DM for a healthy structure is ideally zero, all damages can be detected with a proper setting of the threshold value.

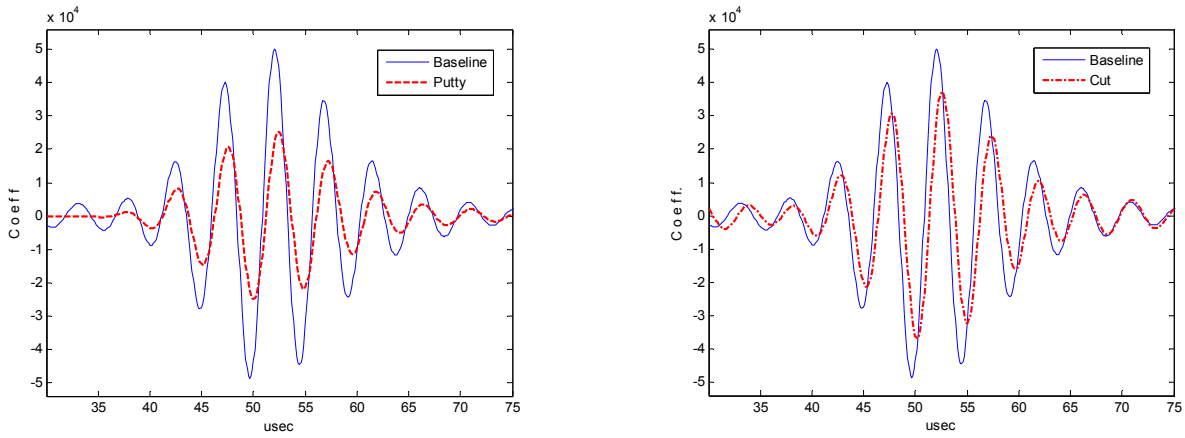

Figure 12: Attenuation of Fundamental Mode Signal S_0 for the Putty and Cut damages

Table 1. Detection Metrics for the Four Damages

Damage	Putty	Notch	Cut	Hole*
DM	0.6438	0.3564	0.6555	0.5041

* The actuator is PZT #1 and sensor is PZT #3 for the hole damage.

Pulse-Echo Experiment:

The objective of our pulse-echo experiment is to measure the distance of the cut damage below PZT #4 shown in Figure 10 (e). The actuator for the experiment is PZT #2, and the sensor is PZT #4. It is important to note that the damage under consideration is not on the path between the two PZT patches, which enables the pulse-echo scheme. First, we captured the baseline waveform between PZT #2 and PZT #4 before introduction of the damage, and the waveform is shown in Figure 13 (a). The first and the second arrival signals are the fundamental synchronous and asynchronous modes S_0 and A_0, respectively. Then, the cut damage was introduced, and the same experiment was repeated. The waveform captured at PZT #4 after the cut is shown in Figure 13 (b).

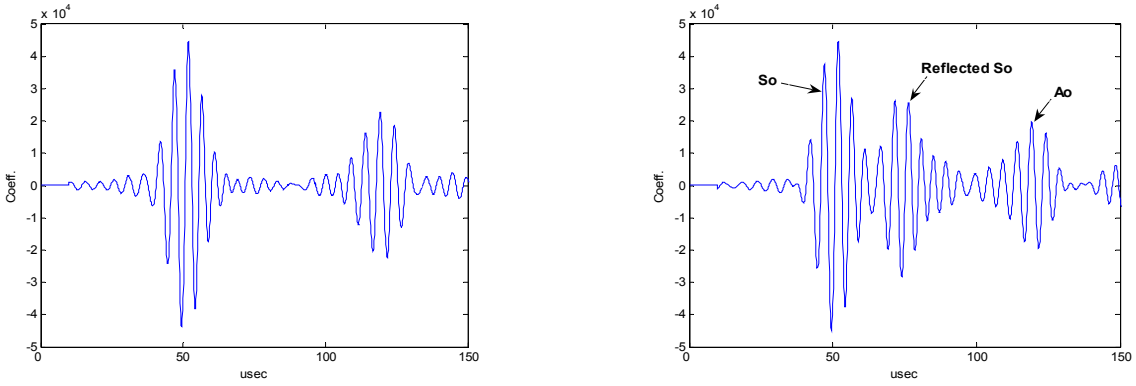

(a) Baseline for the Path between PZT #2 and #4 (b) Sensed at PZT 4 with the Cut Damage

Figure 13: Baseline Waveform and Sensed Echo Waveform as PZT #2 as Actuator and PZT #4 as Sensor

Comparison of the baseline and echoed waveforms shows that the S_0 mode signal is reflected at the cut and trails the original S_0 signal. The difference of the two waveforms is plotted in Figure 14. It is possible to detect the reflected waveform setting a proper threshold value, which may be determined by empirical statistics. The distance of the damage from the sensing PZT #4 can be computed using the time of arrival of the reflected signal and the speed of the fundamental synchronous S_0 mode measured earlier (which is 5080 m/sec). The distance for this particular damage is obtained as 2.5 inches with the amount of error of 0.2 inch.

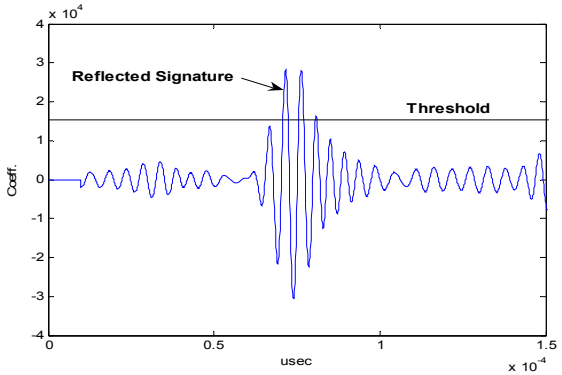

Figure 14: Difference between the Baseline and Echo Waveforms

6. CONCLUSION

We developed an impedance-based SHM method, which performs the SHM operation in digital domain [4]. Our system eliminates a DAC, an ADC, and an FFT operation, which makes the system power efficient and simple in hardware. We incorporated the Lamb wave propagation method into the impedance-based SHM system, in which the DSP processor and the PZT patches are shared. Both pitch-and-catch and pulse-and-echo schemes were implemented for the Lamb wave method. We tested our system for both the impedance and the Lamb wave methods, and experimental results for the Lamb wave method were reported in this paper. The results indicate that our system successfully detects various types of simulated damages on aluminum plates.

ACKNOWLEDGEMENT

We would like acknowledge Extreme Dignostics, Inc, for the financial support to this project. We are also thankful to Dr. Benjamin Grisso, Dr. Seung Hee Park and Mr. Steve Anton with CIMSS at Virginia Tech for their help in the experiments reported in this paper.

REFERENCES

[1] Raghavan, A. and Cesnik, C.E.S., "Review of Guided-wave Structural Health Monitoring" *The Shock and Vibration Digest*, Vol. 39, No. 2, pp. 91-114, (2007)

[2] Park, S., Yun, C.B. and Inman, D.J., "A Self-contained Active Sensor System for Health Monitoring of Civil Infrastructures," *Proceeding of IEEE Sensors Conference*, pp. 798-802 (2006)

[3] Musiani, D., Lin, K. and Rosing, T.S., "Active Sensing Platform for Wireless Structural Health Monitoring," *Proc. of 6th International Symposium on Information Processing in Sensor Networks*, pp. 390-399 (2007)

[4] Kim, J., Grisso, B.L., Ha, D.S. and Inman, D.J., "A system-On-Board Approach for Impedance-Based Structural Health Monitoring," *Proceeding of SPIE,* (2007)

[5] Wait, J.R., Park, G., Sohn, H. and Farrar, C.R., "Plate Damage Identification Using Wave Propagation and Impedance Methods," *Proc. of SPIE*, vol. 5394, pp. 53-65 (2004)

[6] Swartz, R.A., Flynn, E., Backman, D., Hundhausen, R.J. and Park, G., "Active Piezoelectric Sensing for Damage Identification in Honeycomb Aluminum Panels," *Proceedings of 24th Intl. Modal Analysis Conference,* (2006)

[7] Proakis, J.G. and Nanolakis, D.G., [Digital Signal Processing], 4th ed., Prentice Hall, (2007)

[8] Park, G., Sohn, H., Farrar, C.R. and Inman, D.J., "Overview of Piezoelectric Impedance-Based Health Monitoring and Path Forward," *The Shock and Vibration Digest*, vol. 35, Issue 6, pp. 451-463 (2003)

[9] Park, G., Kabeya, K., Cudney, H. H. and Inman, D. J., "Impedance-based structural health monitoring for temperature varying applications," *JSME International Journal*, Series A, vol. 42, pp. 249-258 (1999)

[10] Kim, J., [Low-Power System Design for Impedance-Based Structural Health Monitoring], Ph.D. Dissertation, Virginia Tech, (2007)

[11] Kessler, S.S., [Piezoelectric-based In-situ Damage Detection of Composite Materials for Structural Health Monitoring Systems], Ph.D. Dissertation, MIT, (2002)

[12] Legendre, S., Massicotte, D., Goyette, J. and Bose, T.K., "Wavelet-Transform-Based Method of Analysis for Lamb-Wave Ultrasonic NDE Signals," *IEEE Trans. on Inst. and Meas.*, vol. 49, no. 3, pp. 524-530 (2000)

[13] Sohn, H. Park, G., Wait, J.R., Limback, N.P. and Farrar, C.R., "Wavelet-based active sensing for delamination detection in composite structures," *Journal of Smart Materials and Structures*, vol. 13, pp. 153-160 (2004)

[14] Kim, J., Grisso, B.L., Ha, D.S. and Inman, D.J., "An All-Digital Low-Power Structural Health Monitoring System," *Conference on Technologies for Homeland Security*, pp. 123-128 (2007)